International Journal of Pharmaceutics 612 (2022) 121362

Contents lists available at ScienceDirect

International Journal of Pharmaceutics

journal homepage: www.elsevier.com/locate/ijpharm

Combined sterilization and fabrication of drug-loaded scaffolds using supercritical CO_2 technology☆

Víctor Santos-Rosales [a], Beatriz Magariños [b], Carmen Alvarez-Lorenzo [a], Carlos A. García-González [a,*]

[a] Departamento de Farmacología, Farmacia y Tecnología Farmacéutica, I+D Farma (GI-1645), Faculty of Pharmacy and Health Research Institute of Santiago de Compostela (IDIS), Universidade de Santiago de Compostela, 15782 Santiago de Compostela, Spain
[b] Departamento de Microbiología y Parasitología, Facultad de Biología, CIBUS, Universidade de Santiago de Compostela, 15782 Santiago de Compostela, Spain

ARTICLE INFO

Keywords:
Sterilization
Spores
Supercritical CO_2
Bone scaffold
Technology transfer

ABSTRACT

The access of biodegradable scaffolds to the clinical arena is constrained by the absence of a suitable sterilization technique for the processing of advanced polymeric materials. Sterilization with supercritical CO_2 ($scCO_2$) may circumvent some technological limitations (e.g., low temperature, no chemical residues on the material), although $scCO_2$ can plasticize the polymer depending on the processing conditions used. In this latter case, the integration of the manufacturing and sterilization processes is of particular interest to obtain sterile and customized scaffolds in a single step. In this work, $scCO_2$ was exploited as a concomitantly foaming and sterilizing agent for the first time, developing a one-step process for the production of vancomycin-loaded poly (ε-caprolactone) (PCL) bone scaffolds. The effect of the CO_2 contact time on the sterility levels of the procedure was investigated, and the sterilization efficiency was evaluated against dry spores (*Bacillus stearothermophilus*, *Bacillus pumilus* and *Bacillus atrophaeus)*. Vancomycin-loaded PCL scaffolds had relevant sustained release profiles for the prophylaxis of infections at the grafted area, even those caused by methicillin-resistant *Staphylococcus aureus* (MRSA). The biological performance of the scaffolds was evaluated *in vitro* regarding human mesenchymal stem cells (hMSCs) attachment and growth. Finally, the biocompatibility and angiogenic response of the manufactured sterile scaffolds was assessed *in ovo* through chick chorioallantoic membrane (CAM) assays.

1. Introduction

Sterility is a critical quality attribute of any implantable medical device. At the interface between the implant and the host tissue, the immune system is locally hampered, and thus the clearance of pathogens can be compromised, triggering device-associated infections and biofilm formation on the graft (Rochford et al., 2012). Particularly, periprosthetic joint infections (PJI) represent a significant economic burden for the healthcare system. Only in the USA, the prospective studies of hospital costs for PJI of knee and hip for 2030 year exceed 1.85 billion dollar per year (Premkumar et al., 2021). A combination between aseptic practices and the choice of effective sterilization treatments compatible with the medical device are required to reduce the risk of infection (Josephs-Spaulding and Singh, 2021; Li and Webster, 2017).

The advent in the market of a new generation of biodegradable scaffolds is usually jeopardized by the absence of a sterilization procedure of reference that ensures the stability and performance of the product. Conventional sterilization treatments (steam/heat, ethylene oxide and gamma sterilization) are incompatible with most polymeric biomaterials due to the onset of physicochemical changes once subjected to the harsh sterilization conditions (Tipnis and Burgess, 2018; Zhao et al., 2019).

Carbon dioxide under supercritical conditions ($scCO_2$) has been demonstrated able to inactivate vegetative forms of both Gram-positive and Gram-negative bacteria (Ribeiro et al., 2019). The incorporation of additives such as hydrogen peroxide, ethanol or peracetic acid in low contents results in the successful inactivation of bacterial endospores (Dai et al., 2016; Ribeiro et al., 2019; Soares et al., 2019). The supercritical sterilization can be extended to porous biomaterials for regenerative medicine purposes due to the mild operating conditions and the excellent $scCO_2$ permeability. Recently, the effective sterilization of complex nanostructured biomaterials such as starch aerogels was

☆ The work described in this paper is the subject of patent number ES2808994A1 led by Universidade de Santiago de Compostela.

* Corresponding author.
E-mail address: carlos.garcia@usc.es (C.A. García-González).

https://doi.org/10.1016/j.ijpharm.2021.121362
Received 2 November 2021; Received in revised form 3 December 2021; Accepted 4 December 2021
Available online 9 December 2021

achieved with minor modifications on the textural properties (Santos-Rosales et al., 2019), while ensuring a 6-logarithmic reduction of dry spores of *Bacillus atrophaeus* and *Bacillus stearothermophilus*.

Regarding scaffold manufacturing, polyesters are a family of biodegradable polymers particularly interesting, since their physical and mechanical properties, as well as the degradation rate can be finely tuned by selecting adequate monomer ratios, molecular weights and crystallinity degrees (Makadia and Siegel, 2011; Richbourg et al., 2019). These features allow the manufacturing of scaffolds with specific degradation kinetics and mechanical properties, matching those of the target damaged tissue. Poly(ε -caprolactone) (PCL) shows high strength and resilience which can be advantageous for tissues exposed to moderate mechanical stress, such as tendon, cartilage and bone (Dash and Konkimalla, 2012). Particularly, PCL presents similar mechanical properties to the trabecular bone, which has prompted the development of a variety of scaffolds made of PCL solely or in combination with other polymers (Hedayati et al., 2020; Seddighian et al., 2021; Woodruff and Hutmacher, 2010). PCL-based scaffolds incorporating active pharmaceutical ingredients (APIs) were successfully manufactured through the $scCO_2$ foaming method, matching the morphological and mechanical criteria to be used as trabecular bone replacements (Goimil et al., 2017, 2018; Santos-Rosales et al., 2021a) with promising *in vivo* outcomes (Goimil et al., 2019). To date, several PCL-based scaffolds have reached the market and are commercially available (Osteomesh®, Osteoplug®). However, the simultaneous sterilization and manufacture of scaffolds in a single-step process by using $scCO_2$ is still an ongoing challenge in the field (Dai et al., 2016; Di Maio and Kiran, 2018; Santos-Rosales et al., 2021b).

For the foaming of polymeric scaffolds, temperature, pressure, soaking time and depressurization rate are the main parameters governing the resulting porous architecture (Santos-Rosales et al., 2020b; Chen et al., 2016). When these parameters are individually studied, an increase in the processing temperature favours the formation of scaffolds with larger and more heterogeneous pores. Conversely, when the pressure and soaking time are increased, smaller but more interconnected, abundant and homogeneous pores are obtained (Santos-Rosales et al., 2020a). The depressurization rate was reported to play a critical role in the degree of pore interconnection and the presence of closed pores along the foamed structure (Tai et al., 2007; Chen et al., 2019).

On the other hand, temperature, pressure and soaking time are also critical parameters regarding the sterilization efficacy of $scCO_2$ -based methods (Ribeiro et al., 2019; Santos-Rosales et al., 2021b). The biocidal effect of the $scCO_2$ relies on a combination of multiple mechanisms, where the acidification of cytoplasm and further damage of the cell envelope may play a major role (Ribeiro et al., 2019). In this sense, modifications on these three parameters than enhance the CO_2 solubilization on the bacterial cytoplasm, would increase the sterilization efficacy, i.e. higher pressure, temperature and longer soaking time (Soares et al., 2019). If the integration of both foaming and sterilization processes is aimed, the choice of the operating temperature is particularly challenging since a trade-off solution between the sterilization efficacy and a suitable foam formation must be encountered.

In this work, a one-step sterilization-foaming process based on the $scCO_2$ technology procedure is reported for the first time. The sterility efficacy of the process was assessed against spores from three different biological indicators: *B. atrophaeus*, *B. stearothermophilus* and *B. pumilus*. In parallel, the incorporation of bioactive compounds (vancomycin) to the PCL matrix was also evaluated. The release kinetics of the drug-loaded scaffolds was monitored for 14 days, mimicking a relevant clinical time scenario of infection at the grafted region. The biological performance of the scaffolds was evaluated *in vitro* regarding mesenchymal stem cells (MSCs) attachment and growth. Finally, the biocompatibility and angiogenic response of scaffolds was investigated *in ovo* through chick chorioallantoic membrane (CAM) assays.

2. Materials and methods

2.1. Materials

PCL in the powdered form (50 kDa, T_m = 61.4 °C, 66.7% crystallinity) was supplied by Polysciences (Warrington, PA, USA). Vancomycin hydrochloride (Mw 1486 g/mol, 94.3% purity) was purchased from Guinama (Valencia, Spain). CO_2 (purity of > 99.9%) was employed as foaming and sterilization agent and provided by Nippon Gases (Madrid, Spain). Trypticase soy broth (TSB) and Trypto-casein soy agar (TSA) medium were purchased from BIOKAR Diagnosis (Pantin, France) and hydrogen peroxide 30% (v/v) from Sigma-Aldrich (Madrid, Spain). Water was purified using reverse osmosis (resistivity > 18 MΩ·cm, MilliQ, Millipore, Madrid, Spain). Sterilization reel was purchased from E-line S.r.l. (Torre Pallavicina, Italy).

2.2. Screening of the supercritical sterilization conditions

Commercial spore strips with 10^6 spores of *B. stearothermophilus* (ATCC 7953) and *B. pumilus* (ATCC 27142) were purchased from Sigma-Aldrich (Madrid, Spain). *B. atrophaeus* (cell line 9372) spores were obtained from Crosstex International (Rush, NY, USA). These three microorganisms are the biological indicators used in steam and hydrogen peroxide vapor sterilization, radiation sterilization (ISO 11137–1:2006/*Amd.1:2013*) and ethylene oxide or dry heat sterilization (ISO 11135:2014), respectively. The spore strips were sealed and placed in a 100 mL-stainless steel autoclave (Thar Process, Pittsburg, PA, USA) equipped with a top agitation system (700 rpm), including 1200 ppm of H_2O_2 as additive. The autoclave was then heated to 39 °C and pressurized until 140 bar at a constant pressurization rate of 13.3 bar/min and a continuous flow of CO_2 at 5 g/min was maintained for the desired period time (1 to 5 h, Table 1). Finally, the system was depressurized at a constant venting rate of 3 bar/min until atmospheric pressure.

Bacterial growth was visually evaluated through turbidity tests (inspection by naked eye) after 7 and 14 days of incubation without stirring (Raypa Digital Incubators, Terrassa, Spain) of the strips in tubes containing 10 mL of TSB liquid medium, under the corresponding recommended incubation temperatures of 37 °C (*B. pumilus* and *B. atrophaeus*) and 60 °C (*B. stearothermophilus*) (Fig. S1). In addition, the absence of growth was verified by seeding 1 mL of the studied tubes after 7 and 14 days in TSA plates.

2.3. One-step $scCO_2$ sterilization and foaming of PCL scaffolds

PCL or PCL-vancomycin 5 wt% (denoted as PCL-V) powders (1.5 g) were poured in cylindrical Teflon moulds (L: 24.6 mm, D: 17 mm) (Brand GmbH, Wertheim, Germany), manually mixed with a spatula and further compacted with an aluminium plunger. The moulds containing the samples were packed in individual sterilization reel pouches thermally sealed and then placed in a 100-mL stainless steel reactor (Thar Process, Pittsburg, PA, USA). Hydrogen peroxide (commercial H_2O_2 solution 30% v/v) was added at the bottom of the autoclave targeting 1200 ppm with respect to the volume of the autoclave per test. To avoid the physical contact of the samples with the additive before reaching

Table 1
Dynamic $scCO_2$ sterilization tests of bacterial endospores at 39 °C, 140 bar and in presence of 1200 ppm of H_2O_2. Notation: Y denotes that 6-logarithmic reductions (logR-6) were reached for the specific *Bacillus* strain.

Test	$scCO_2$ continuous flow duration (h)	Spore sterilization efficacy (logR-6)		
		B. stearothermophilus	*B. pumilus*	*B. atrophaeus*
#1	1	–	–	Y
#2	2	Y	–	Y
#3	2.5	Y	Y	Y
#4	5	Y	Y	Y

supercritical conditions, samples were placed on top of an aluminium platform. Afterwards, the system was subjected to the test #3 processing conditions (Table 1). Scaffolds in the form of cylindrical foams were collected from the autoclave and stored for further characterization.

2.4. Structural and physicochemical characterization of PCL-based scaffolds

Morphologies and surface texture of the scaffolds were analyzed by scanning electron microscopy (FESEM, ULTRA PLUS, Zeiss, Oberkochen, Germany) running at 10 kV. Scaffolds were sliced with a scalpel and then iridium-sputtered (10 nm thickness), prior to their imaging.

A digital caliper (Fowler™, Newton, MA, USA) was used to measure the dimensions of the cylindrical scaffolds, and their bulk densities (ρ_{bulk}) were calculated from the volume and weight. A helium pycnometer (Quantachrome, Boynton Beach, FL, USA) was used to determine the skeletal density (ρ_{skel}) from six replicates at room temperature (25 °C) and a pressure of 1.01 bar. Overall porosity (ε) was calculated from Equation (1):

$$\varepsilon(\%) = \left(1 - \frac{\rho_{bulk}}{\rho_{skel}}\right) x100 \quad (1)$$

Mercury intrusion porosimetry (MIP) analyses of the scaffolds were performed (Autopore IV 9500 model, Micromeritics, Norcross, GA, USA) at working pressures ranging from 0.07 to 1800 bar to determine their pore size distributions. Porosity values (ε_{MIP}) were determined from the intruded volume of mercury ($V_{p_{MIP}}$) in the scaffolds with the increase of pressure using the Washburn equation (Ho and Hutmacher, 2006).

Physicochemical changes of vancomycin due to the $scCO_2$ treatment was studied by X-ray diffraction (XRD) and Attenuated Total Reflectance/Fourier-Transform Infrared spectroscopy (ATR/FT-IR). Crystallinity of the raw and treated drug was studied by XRD (PW-1710, Philips, Eindhoven, The Netherlands) in the 2–50° 2θ-range using a 0.02° step and Cuκα$_1$ radiation. ATR/FT-IR analysis was performed using a Gladi-ATR accessory equipped with a diamond crystal (Pike, Madison, WI, USA). Raw and $scCO_2$-treated vancomycin were characterized in the mid-IR spectrum range (400 – 4000 cm^{-1}) using 32 scans at a resolution of 2 cm^{-1}.

2.5. Vancomycin release studies and antimicrobial effect

Scaffolds cut in pieces of 100 mg of weight were immersed in tubes containing 25 mL of PBS pH 7.4 as release medium and put in an oscillating bath (Unitronic 320 OR, Selecta, Barcelona, Spain) at 37 °C and 60 rpm for 14 days. Aliquots of 3 mL were collected at selected time periods (0.5, 1, 2, 4, 8, 24, 48, 122, 170, 218 and 360 h). The extracted volume was replaced with fresh PBS medium. Vancomycin concentration was measured by UV–Vis spectrophotometry (8453 model, Agilent Technologies, Santa Clara, CA, USA) at a wavelength of 281 nm. Vancomycin standard solutions were prepared in PBS medium at concentrations in the 20–200 μg/mL range and in triplicate. Release studies were conducted in triplicate maintaining sink conditions medium (i.e. concentrations at least 10 times lower than the maximum drug solubility, 100 mg/mL (López-Iglesias et al., 2020)).

The modelling of the vancomycin release kinetics was fitted to a biexponential equation (Eq. (2)) referring to two simultaneous first-order dissolution processes using GraphPad Prism v.6.04 for Windows software (GraphPad Software, San Diego, CA, USA).

$$D = D_{max,1}\left(1 - e^{-k_1 t}\right) + D_{max,2}\left(1 - e^{-k_2 t}\right) \quad (2)$$

where D denotes the dosage percentage of vancomycin released at time t, in %; $D_{max,i}$ is the maximum dosage percentage of vancomycin released in stage i, in %; and k_i is the release rate coefficient in stage *i*, in h^{-1} (García-González et al., 2018).

On the other hand, the antimicrobial activity of the vancomycin released from the scaffolds was proven as follows. Briefly, 10 mL tubes containing TSB were inoculated with *Staphylococcus aureus* (ATCC 25923) and, simultaneously, 100 mg of scaffold pieces (PCL and PCL-V) were placed in the tubes. After the procedure, tubes were incubated under agitation (200 rpm) at 37 °C for 24 h and cell growth was evaluated by visual inspection of the turbidity of the medium.

2.6. Cytotoxicity, cell proliferation and adhesion tests

Human mesenchymal stem cells derived from bone marrow (hMSC; ATCC PCS-500–012) were used to evaluate the cytotoxicity of the manufactured scaffolds. Briefly, cells were seeded in 24-well plates (20,000 cells/well, passage 5) with 2 mL of culture medium: αMEM supplemented with 20% FBS and 1% penicillin (10,000 UI/mL)/streptomycin (10,000 μg/mL). Cells were maintained overnight at 37 °C in a humidified atmosphere enriched with 5% CO_2 to allow their attachment to the bottom of the well. Since PCL is highly hydrophobic (Woodruff and Hutmacher, 2010), scaffold pieces (50 mg) were immersed in the supplemented medium prior to seeding to ensure their contact with cells. Scaffolds were incubated with cells in triplicate for 24 h at the former conditions. Controls included cells incubated without scaffolds.

Cell viability was evaluated using the cell counting kit-8 (CCK-8) (Roche, Switzerland) at 24 h and performed according to the manufacturer protocol. Absorbance was read at 450 nm (UV BioRad Model 680 microplate reader, Hercules, CA, USA). Experiments were carried out in quintuplicate and the cell viability (%) calculated as follows:

$$Cell\ viability\ (\%) = \frac{Abs_{exp}}{Abs_{negative\ \ control}} \times 100 \quad (3)$$

Cell proliferation was analyzed at 6 and 14 incubation days with the following seeding protocol. Scaffold cubic pieces were placed in a plastic syringe containing supplemented medium with a cellular density of 70,000 cells/scaffold. During 4 h, syringes where rotated every 30 min. Afterwards, scaffolds were placed in 24-well plates with 2 mL of culture medium. At the sampling periods, the scaffolds were washed with PBS and processed for microscopy analysis in triplicate. To evaluate the growth and attachment of hMSCs, scaffolds were stained following standard protocols with phalloidin/4,6-diamine-2-phenylindole (DAPI, Thermofisher Scientific, Waltham, MA, USA) to visualize the cytoplasm and nuclei of cells, respectively. Briefly, MSCs seeded on the scaffolds were fixed in paraformaldehyde (4 % (w/v)) for 10 min at room temperature. After washing with PBS, cells were permeabilized with 0.1 % (v/v) Triton/PBS for 5 min, washed again and incubated in darkness for 30 min with Alexa Fluor-488® dye (Thermofisher Scientific, Waltham, MA, USA). Finally, scaffolds were washed again with PBS and one drop of DAPI was added to each sample. Scaffolds were visualized with a Leica TCS-SP2 spectral confocal microscope (Leica TCS-SP5, Leica Microsystems Heildelberg GmbH, Mannheim, Germany).

2.7. Scaffold biocompatibility and angiogenic response on chick chorioallantoic membrane (CAM)

The CAM assay was used to evaluate the biocompatibility of the scaffolds ($n = 3$) as well as *in vivo* angiogenesis. The studies were carried out using a previously reported procedure (Mangir et al., 2019) not requiring ethics committee approval (Spanish Government Regulation RD 53/2013). Fertilized hen eggs obtained from Coren (Ourense, Spain) were incubated at 37 °C and 60 % RH for several days. At day 3, a small portion of the shell was removed under sterile conditions to verify the fertilization of the eggs and the embryo development. At day 8, scaffolds were directly placed on the CAM of the egg and incubated until early day 14, to study material integration on the CAM and the new vessel formation (Moreno-Jiménez et al., 2017). The surrounding membrane was carefully cut and scaffolds removed from the eggs. To better visualize angiogenesis, membranes were fixed in a paraformaldehyde solution (4 % (w/v), 10 min) and placed in a Petri dish with PBS under a 48 MPx

wide-angle lens (Xiaomi Mi9SE, Xiaomi Inc., Beijing, China) and pictures were taken.

2.8. Statistical analysis

Results were expressed as mean ± standard deviation. One-way ANOVA followed by the post hoc Tukey HSD multiple comparison tests were performed for the density values of the scaffolds using Statistica v8.0 software (StatSoft Inc., Tulsa, OK, USA).

3. Results and discussion

3.1. Screening of the sc-sterilization conditions compatible with the sc-foaming

As a first step, previous to the design of the scaffold manufacturing method, the feasible operating window of sc-sterilization processing parameters under a continuous CO_2 flow regime leading to 6-logarithmic reduction (logR-6) of dry spores was explored. The inactivation of 10^6 resistance microorganisms was targeted since it is the sterility level to be reached according to the current legal framework for the sterilization of medical devices (ISO 14937:2009).

The processing temperature (39 °C) and pressure (140 bar) were set according to the promising morphological features of PCL-based foams previously reported by our research group (Goimil et al., 2017, 2019; Santos-Rosales et al., 2021a, 2020a). Under these or similar conditions of pressure and temperature, there is a paucity of information of the sterilization efficacy of $scCO_2$ either solely or in combination with additives against bacterial endospores (Ribeiro et al., 2019). For instance, the reported operating conditions achieving logR-6 against dry spores of *B. pumilus, B. atrophaeus* and *B. stearothermophilus* are close to 270 bar of pressure and 40–60 °C range of temperature, always in presence of additives (Zhang et al., 2006b, 2006a; Donati et al., 2012).

H_2O_2 (1200 ppm) was added in the liquid form at the bottom of the autoclave for the sterilization tests to enhance the biocidal activity of $scCO_2$ against dry spores of *Bacillus* genus species (Zhang et al., 2006a, 2006c). The effect of the CO_2 contact time under a continuous CO_2 flow of 5 g/min on the sterility level of the treated materials was then investigated.

Complete inactivation of *B. atrophaeus* spores was achieved after 1 h of processing (test #1, Table 1). Based on the results obtained with these spores, the abovementioned working parameters may be potentially extrapolated for the inactivation of vegetative forms of a wide variety of bacterial strains (both Gram-positive and Gram-negative), and viruses (non-enveloped or enveloped), according to its resistance to sterilization treatments (Dai et al., 2016) and particularly to $scCO_2$-based methods (Ribeiro et al., 2019; Zhang et al., 2006c).

A further increase of the contact time to 2 h was only effective against *B. stearothermophilus* and *B. atrophaeus*, whilst the *B. pumilus* spore strain grew in the first 24 h post-treatment (test #2). Finally, a duration of 2.5 h or longer was required to achieve the logR-6 for the three tested biological indicators (tests #3 and #4). The higher resistance of *B. pumilus* spores to the $scCO_2$ sterilization with H_2O_2 as additive was previously reported (Shieh et al., 2009; Zhang et al., 2006a) and this spore strain has been proposed as the "biological indicator" for monitoring $scCO_2$ sterilization methods (Santos-Rosales et al., 2021b).

The development of a $scCO_2$-based sterilization protocol strictly based on a continuous CO_2 flow was a complete success to reach logR-6 levels for spores. Traditionally, the employment of semi-continuous regimes or of pressure cycles was reported to enhance the sterilization efficacy, but the biocidal activity of $scCO_2$-H_2O_2 admixtures was mainly attributed to the static stage (Checinska et al., 2011; Shieh et al., 2009). Namely, the two-stage inactivation kinetics of *B. pumilus* spores in $scCO_2$ medium containing H_2O_2 was attributed to the formation of a protective barrier of the firstly killed spores followed by a second stage where $scCO_2$ must diffuse through them to reach the pending spores to be inactivated (Checinska et al., 2011). In this context, the dynamic procedure might facilitate the access of the $scCO_2$-H_2O_2 mixture by displacing the dead cells, thus allowing for higher penetration. The $scCO_2$ flow might also accelerate the extraction of membrane components from the bacteria (Garcia-Gonzalez et al., 2007). To the best of our knowledge, this work reports for the first time the achievement of logR-6 levels against spores of the three different biological indicators based on a dynamic procedure.

Moreover, the dynamic sterilization strategy also resulted in an efficient approach to remove H_2O_2 residues in the treated materials, which can be potentially hazardous (Watt et al., 2004). Dry commercial spore strips were obtained after being subjected to the sterilization procedure. However, process durations lower than 2 h rendered liquid H_2O_2 residues at the bottom of the autoclave. Overall, the optimized dynamic conditions (test #3, Table 1) provided not only an efficient sterilization but also an aeration step by itself, ensuring hydrogen peroxide-free materials.

3.2. Manufacturing of sterile and drug-loaded PCL scaffolds in a single-step

The optimized parameters for sterilization (test #3, Table 1) were employed for the supercritical foaming of porous PCL scaffolds. Sterile and highly porous (>74 %) scaffolds were obtained after 2.5 h of contact with a constant CO_2 flow (Table 2). The chemical identity of the raw materials was not affected during the scaffold fabrication according XRD and FTIR analyses (Fig. S2). After the procedure, dry scaffolds were collected and no visible liquid residues of H_2O_2 were found at the bottom of the autoclave. The formation of a thin skin was observed on the scaffold surface, characteristic of supercritical CO_2 foamed structures (Santos-Rosales et al., 2020a). Porosity evaluated from MIP-measurements represented over 50% of the overall porosity values (Table 2). These values indicate that scaffolds presented a relevant open pore population ranging from 0.01 to 180 μm. The presence of micropores (<10 μm) was reported to generate rough surfaces that facilitate the cell attachment and the penetration of body fluids (Diaz-Rodriguez et al., 2018). On the other hand, the presence of a high fraction of large and interconnected pores in the 100–600 μm range was detected by SEM microscopy (Fig. 1), falling in the ideal range for bone tissue engineering (Abbasi et al., 2020; Baino et al., 2016). In the case of vancomycin-loaded scaffolds (PCL-V), the structures were lighter than pure PCL scaffolds (Table 2), although differences were not significant ($p < 0.05$) and the porous morphology was almost identical.

3.3. Vancomycin release from the sterile PCL scaffolds

Vancomycin is a long-standing used broad-spectrum antibiotic, active against Gram-positive bacteria and currently of clinical choice for infections caused by methicillin-resistant *Staphylococcus aureus* (MRSA) (Cong et al., 2020). Particularly, *S. aureus* is the most common pathogen in periprosthetic joint infections and the parenteral use of vancomycin is frequent (Yang et al., 2018). However, the side-effects of vancomycin encourage its local administration to achieve therapeutic levels while avoiding the nephrotoxicity and ototoxicity of this drug. Therefore, PCL scaffolds incorporating vancomycin might not only support the regeneration of native bone, but also prevent the outbreak of infections at the

Table 2
Physicochemical properties of the foamed and sterile PCL-scaffolds processed with $scCO_2$ at 39 °C, 140 bar with addition of 1200 ppm of H_2O_2 and operating in the dynamic mode (5 g CO_2/min for 2.5 h).

Scaffold	ρ_{bulk} (g/cm^3)	ρ_{skel} (g/cm^3)	ε (%)	ε_{MIP} (%)
PCL	0.290 ± 0.002*	1.141 ± 0.007*	74.6 ± 0.2	46.24
PCL-V	0.276 ± 0.006*	1.128 ± 0.006*	75.5 ± 0.5	43.58

* Statistically homogeneous (1-way ANOVA, $p < 0.05$).

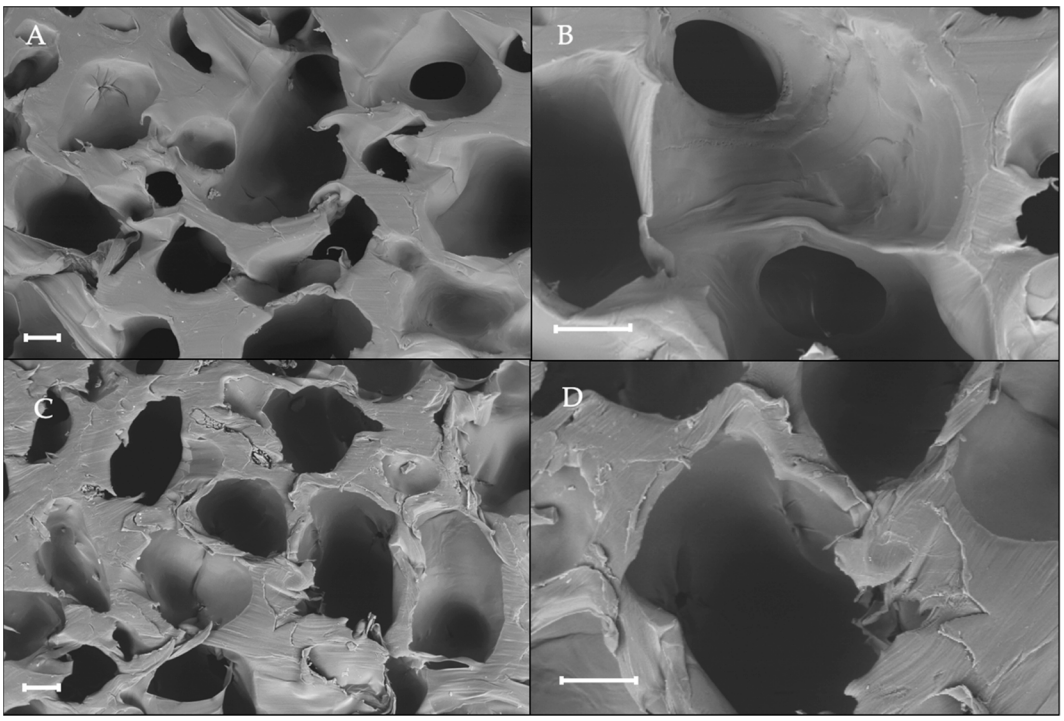

Fig. 1. SEM images of cross-sections of (A, B) PCL and (C, D) PCL-V scaffolds obtained according to test #3 (in Table 1) operating conditions. Scale bars: 200 μm.

grafted area.

The $scCO_2$ scaffold treatment did not modify the chemical identity of the vancomycin hydrochloride salt, according to XRD and FTIR analyses (Fig. S3). Vancomycin hydrochloride is highly soluble in water (200 mg/mL) (Li et al., 2010). Accordingly, pure vancomycin in the powdered form was almost completely dissolved (89.2 ± 3.2 %) in the first 15 min (data of the dissolution test not shown). Vancomycin incorporation in the PCL matrix (PCL-V scaffolds) resulted in release profiles displaying a two-stage pattern. Firstly, a burst release representing close to 20% of the loaded drug was observed in the first 8 h (Fig. 2, right), whilst a sustained release was achieved for over 2 weeks (Fig. 2, left). After 2 weeks, only half of the total vancomycin payload was released to the medium. Due to the strong interaction with the polymeric matrix, the remaining drug might be released concomitantly with PCL degradation.

Vancomycin release profile was fitted to a bi-exponential drug release model (Eq. (2)) (Table 3). The accuracy of the fitting refers to a profile with a stepwise dissolution of two vancomycin fractions. Firstly, the vancomycin weakly interacting with the PCL was released through a dissolution process and was the main responsible for the burst release. Then, a deeply interacting vancomycin fraction was released by dissolution/diffusion from the polymeric matrix to the medium. A similar bi-exponential drug release pattern was previously obtained for PCL scaffolds containing vancomycin and chitosan in different weight ratios (García-González et al., 2018).

Table 3
Kinetic fitting parameters of the vancomycin release profile from PCL-V scaffolds according to Eq. (2).

D_{max1}, dose %	$k_1(10^{-3})$, h^{-1}	D_{max2}, dose %	k_2, h^{-1}	R^2
29.76 ± 1.78	7.07 ± 1.10	18.97 ± 0.74	1.291 ± 0.18	0.9946

The designed and manufactured drug-loaded scaffolds presented relevant release profiles for the prophylaxis and treatment of infections at the grafted area. Namely, the minimal inhibitory concentrations (MIC) of vancomycin against *S. aureus* were established by Clinical & Laboratory Standards Institute (CLSI), in the 2–16 μg/mL range depending on the resistance of the strain (Al-Marzoqi et al., 2020; Martinez et al., 2009). Assuming a similar behavior in an *in vivo* environment, PCL-V scaffolds ensured an early effective vancomycin release of > 20 μg/mL at the first release times (60 min) under the experimental setup conditions (25 mL), thus beyond the abovementioned MIC-

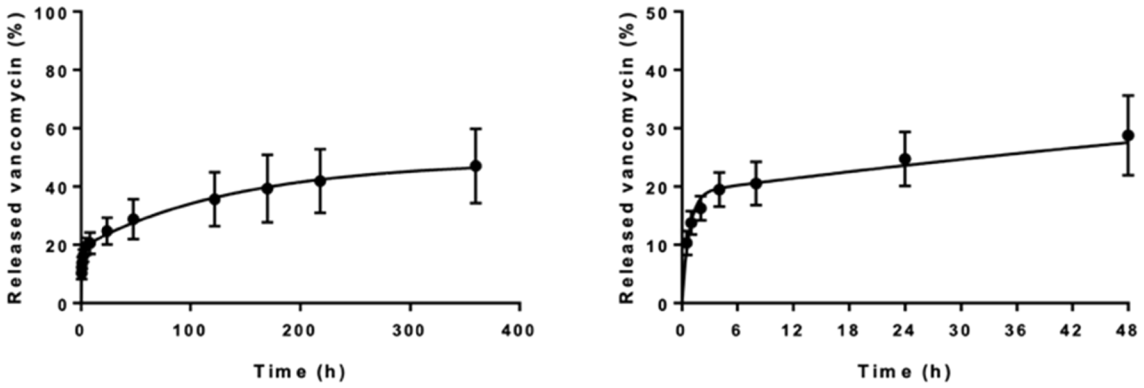

Fig. 2. Vancomycin release profile from PCL-V scaffolds in PBS pH 7.4, 37 °C and 60 rpm for 14 days (left) and close up during the first 48 h (right).

threshold. In addition, the antimicrobial activity of the vancomycin-loaded scaffolds (PCL-V) was confirmed after 24 h of incubation with *S. aureus* and monitored with their unmedicated counterparts (Fig. S4).

3.4. Cytocompatibility of the scaffolds and in vitro performance

Scaffolds were directly collected from the autoclave in their individual packaging (thermally sealed sterilization pouches) and subjected to the biological tests. The absence of microbial growth through the assays confirmed the sterility of the material and highlighted its ease of storage and further handling in clean environments. The cytocompatibility of the material with hMSCs was tested at 24 h as a proof-of-concept before undergoing more sophisticated experiments. hMSCs in contact with the scaffolds grew in the same extent as for the negative control (cells without material) (Fig. S5). Thus, the developed dynamic process did not only ensure the manufacturing of sterile PCL scaffolds, but also served as an efficient strategy to avoid cytotoxic H_2O_2 residues trapped in the scaffolds, which are known to be cytotoxic even at low concentrations (1 μM) (Stone and Yang, 2006).

Adhesion tests of hMSCs on PCL-scaffolds were performed at 6 and 14 days of incubation to assess the feasibility of the porous material to be used as bone scaffolds. hMSCs presence on the scaffold surfaces was observed after 6 days (Fig. 3A,C). Cells presented a good morphology with elongated cytoplasm, although not in a large quantity (Fig. 3). Cells were observed after 14 days of incubation, verifying the manufactured scaffolds ensured the hMSCs survival (Fig. 3B,D), while no signs of cellular differentiation were detected. PCL-V scaffolds (Fig. 3C,D) presented a similar biological behaviour than their non-medicated counterparts (Fig. 3A,B).

CAM tests were used to provide information regarding safety and biocompatibility as well as to assess the angiogenic activity of biomaterials. Since the circulatory system of the chick embryo and the CAM are connected, the presence of toxic scaffolds can alter the normal development of the chick (Moreno-Jiménez et al., 2017). In this context, all specimens showed good development and all the CAM eggs ($n = 3$) arrived at the end-point of the assay, pointing to the absence of toxicity of the manufactured scaffolds.

The tested scaffolds (PCL and PCL-V) showed high integration to the CAM. For instance, material was recovered only by carefully removing the surroundings of the CAM to avoid its rupture.

Scaffolds must support the ingrowth of blood vessels in order to be integrated and assist the regeneration of the host tissue (García-González et al., 2015). Namely, the absence of nutrients and oxygen in tissue engineered constructs leads to cell damage and death, hampering the suitable scaffold performance once grafted (Serbo and Gerecht, 2013). The top and bottom surfaces of the scaffolds displayed a different aspect (Fig. 4). The bottom surfaces (B in Fig. 4) of the scaffolds were in direct contact with the CAM, whilst the top (T in Fig. 4) of the material not. These visual differences were more likely due to the dimensions of the material (*ca.* 2.5 mm height) instead of the lack of interaction with the membrane (Mangir et al., 2019). The reduction on the dimensions of the tested material would probably render identical surfaces. For the bottom parts of the scaffolds, blood vessels were observed within the matrix suggesting an appropriate integration and interplay of the

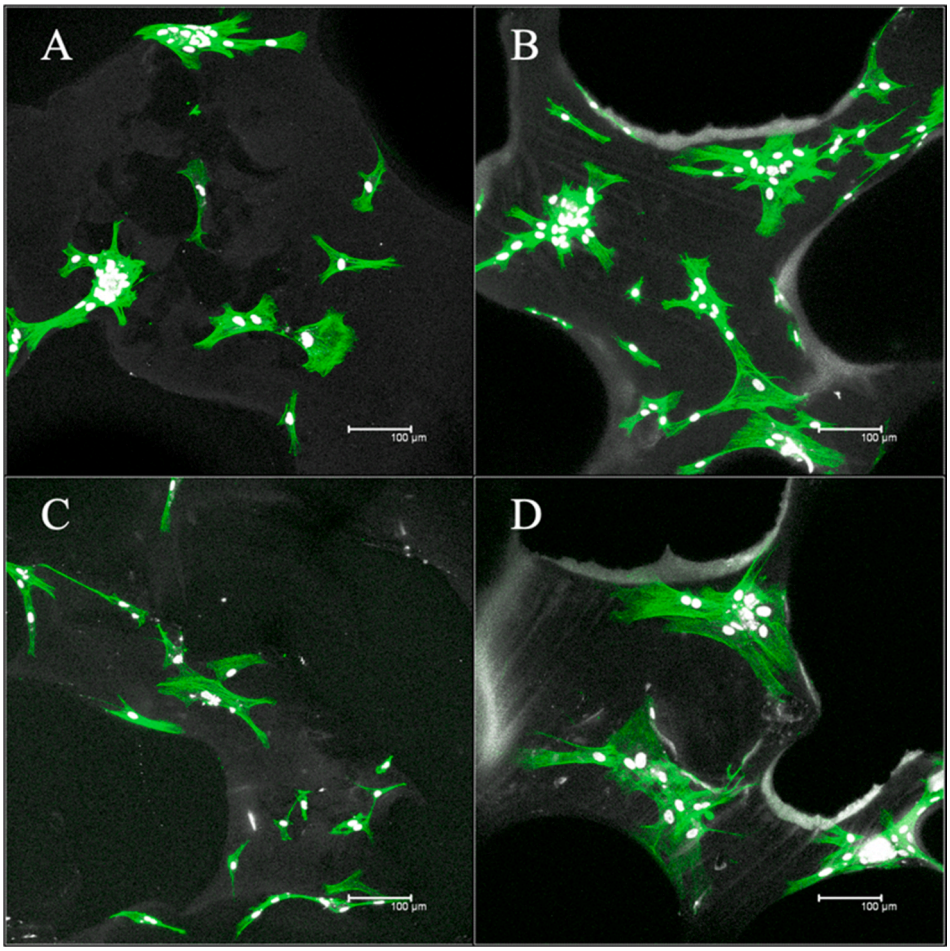

Fig. 3. Confocal microscopy images of hMSCs adhesion and growth on (A, B) PCL and (C, D) PCL-V scaffolds after (left) 6 and (right) 14 days of incubation. Cells were stained with Alexa Fluor-488® dye (cytoplasm, in green) and DAPI (nuclei, in white). (For interpretation of the references to colour in this figure legend, the reader is referred to the web version of this article.)

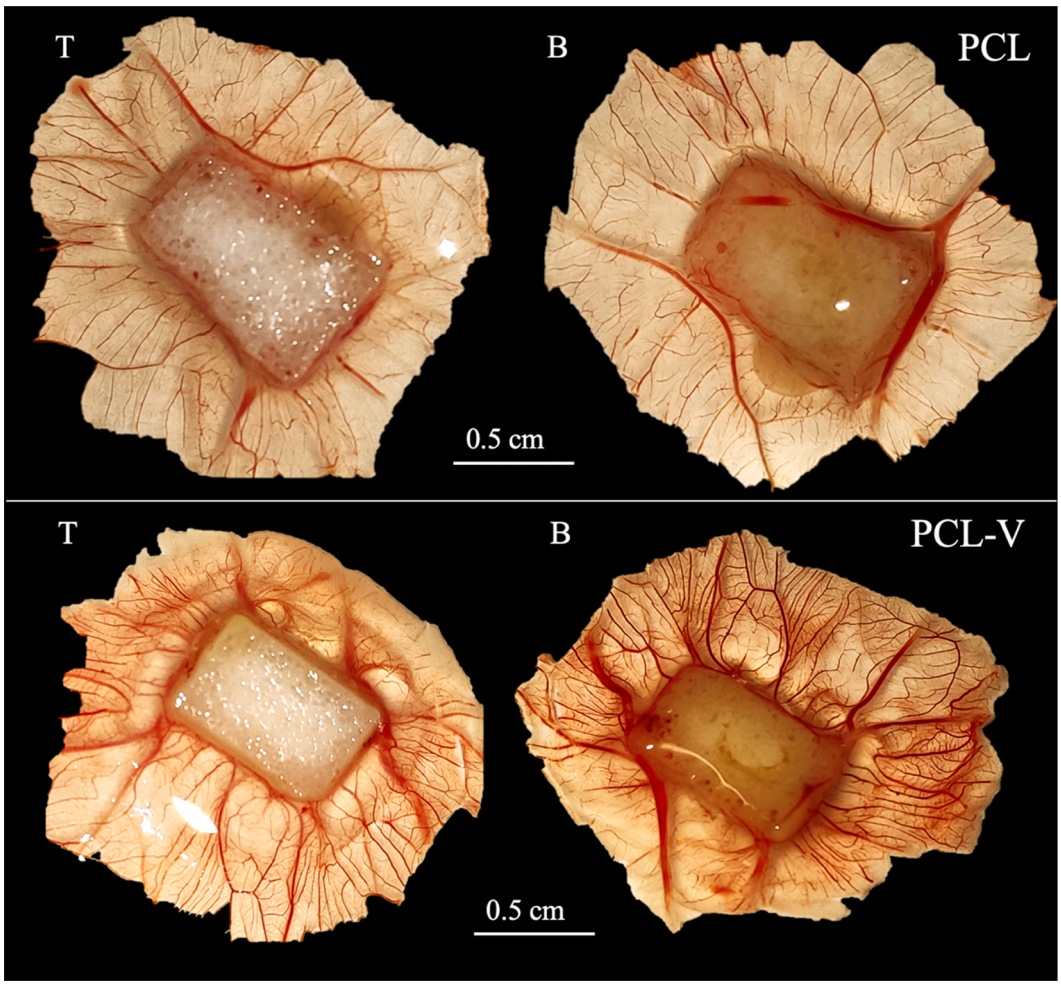

Fig. 4. Representative images of CAM results at early day 14 of the embryonic development. The biocompatibility and angiogenic properties of PCL-based scaffolds was evaluated. Notation: T indicates top surface of the scaffolds, while B refers to the bottom surface in direct contact with the CAM.

scaffolds with the CAM (Fig. 4, right). Coherently, the blood vessels crossing the scaffold could also be detected in the top surfaces (Fig. 4, left). Qualitatively, scaffolds incorporating vancomycin (PCL-V) seemed to present higher degree of vascularization compared to their unmedicated counterparts (PCL). No signs of haemorrhage were observed for PCL-V samples, whilst non-specific immune reactions cannot occur since immune system of the embryo is not yet developed (Ribatti, 2016), discarding an irritation effect of the vancomycin.

4. Conclusions

A simultaneous manufacturing and sterilization method for scaffolds is herein reported for the first time. The integration of both processes may overcome some of the major technological limitations hampering scaffold development towards clinical use. Sterile PCL scaffolds with morphological features similar to natural bone tissue were obtained using $scCO_2$ technology. To the best of our knowledge, this work also represents the first report achieving logR-6 sterilization levels against dry spores based on a dynamic procedure. This approach resulted in H_2O_2-free scaffolds without requiring post-processing aeration steps. In addition, the incorporation of a drug of interest for the treatment of orthopaedic-surgical infections (vancomycin) in the sterile PCL scaffolds was achieved, preserving its chemical identity. The medicated scaffolds (PCL-V) presented a relevant release pattern for the prophylaxis and treatment of infections at the grafted area. Regarding the biological performance, scaffolds supported the MSCs attachment and growth without inducing their differentiation towards a specific cell line. Moreover, *in ovo* results proved the biocompatibility, safety and vascularization of the scaffolds. Overall, this novel method allowed for the production of sterile and medicated PCL scaffolds with promising features for bone regeneration. These scaffolds are obtained in individual packages, which facilitates its handling and storage as ready-to-implant scaffolds. Due to the mild processing temperatures required, the sterilization and manufacturing of polymeric scaffolds incorporating thermolabile compounds such as monoclonal antibodies might be feasible.

CRediT authorship contribution statement

Víctor Santos-Rosales: Conceptualization, Investigation, Methodology, Writing – original draft, Writing – review & editing. **Beatriz Magariños:** Conceptualization, Formal analysis, Methodology, Writing – original draft, Writing – review & editing. **Carmen Alvarez-Lorenzo:** Funding acquisition, Writing – original draft, Writing – review & editing. **Carlos A. García-González:** Conceptualization, Funding acquisition, Methodology, Supervision, Writing – original draft, Writing – review & editing.

Declaration of Competing Interest

The authors declare that they have no known competing financial interests or personal relationships that could have appeared to influence the work reported in this paper.

Acknowledgments

This research was funded by Xunta de Galicia [ED431C 2020/17], MICINN [PID2020-120010RB-I00], Consellería de Sanidade, Servizo Galego de Saúde, Axencia de Coñecemento en Saúde (ACIS, CT850A-G), Agencia Estatal de Investigación [AEI] and FEDER funds. V. Santos-Rosales acknowledges to Xunta de Galicia (Consellería de Cultura, Educación e Ordenación Universitaria) for a predoctoral research fellowship [ED481A-2018/014]. Authors wish to acknowledge the support of Dr. Inés Ardao with the modelling of the vancomycin release kinetics.

Appendix A. Supplementary data

Supplementary data to this article can be found online at https://doi.org/10.1016/j.ijpharm.2021.121362.

References

Abbasi, N., Hamlet, S., Love, R.M., Nguyen, N.-T., 2020. Porous scaffolds for bone regeneration. J. Sci. Adv. Mater. Devices 5 (1), 1–9. https://doi.org/10.1016/j.jsamd.2020.01.007.

Al-Marzoqi, A.H., Kareem, S.M., Alhuchaimi, S., Kadhim Hindi, N.K., Ghasemian, A., 2020. Decreased vancomycin susceptibility among Staphylococcus aureus clinical isolates and postulated platforms to explore rational drugs. Rev. Med. Microbiol. 31, 111–116. https://doi.org/10.1097/MRM.0000000000000204.

Baino, F., Fiorilli, S., Vitale-Brovarone, C., 2016. Bioactive glass-based materials with hierarchical porosity for medical applications: Review of recent advances. Acta Biomater. 42, 18–32. https://doi.org/10.1016/j.actbio.2016.06.033.

Checinska, A., Fruth, I.A., Green, T.L., Crawford, R.L., Paszczynski, A.J., 2011. Sterilization of biological pathogens using supercritical fluid carbon dioxide containing water and hydrogen peroxide. J. Microbiol. Methods 87 (1), 70–75. https://doi.org/10.1016/j.mimet.2011.07.008.

Chen, C.-X., Liu, Q.-Q., Xin, X., Guan, Y.-X., Yao, S.-J., 2016. Pore formation of poly (ε-caprolactone) scaffolds with melting point reduction in supercritical CO_2 foaming. J. Supercrit. Fluids 117, 279–288. https://doi.org/10.1016/j.supflu.2016.07.006.

Chen, C.-X., Peng, H.-H., Guan, Y.-X., Yao, S.-J., 2019. Morphological study on the pore growth profile of poly(ε-caprolactone) bi-modal porous foams using a modified supercritical CO_2 foaming process. J. Supercrit. Fluids 143, 72–81. https://doi.org/10.1016/j.supflu.2018.07.029.

Cong, Y., Yang, S., Rao, X., 2020. Vancomycin resistant Staphylococcus aureus infections: A review of case updating and clinical features. J. Adv. Res. 21, 169–176. https://doi.org/10.1016/j.jare.2019.10.005.

Dai, Z., Ronholm, J., Tian, Y., Sethi, B., Cao, X., 2016. Sterilization techniques for biodegradable scaffolds in tissue engineering applications. J. Tissue Eng. 7, 204173141664881. https://doi.org/10.1177/2041731416648810.

Dash, T.K., Konkimalla, V.B., 2012. Poly-ε-caprolactone based formulations for drug delivery and tissue engineering: A review. J. Controlled Release 158 (1), 15–33. https://doi.org/10.1016/j.jconrel.2011.09.064.

Di Maio, E., Kiran, E., 2018. Foaming of polymers with supercritical fluids and perspectives on the current knowledge gaps and challenges. J. Supercrit. Fluids 134, 157–166. https://doi.org/10.1016/j.supflu.2017.11.013.

Diaz-Rodriguez, P., Sánchez, M., Landin, M., 2018. Drug-Loaded Biomimetic Ceramics for Tissue Engineering. Pharmaceutics 10, 272. https://doi.org/10.3390/pharmaceutics10040272.

Donati, I., Benincasa, M., Foulc, M.-P., Turco, G., Toppazzini, M., Solinas, D., Spilimbergo, S., Kikic, I., Paoletti, S., 2012. Terminal Sterilization of BisGMA-TEGDMA Thermoset Materials and Their Bioactive Surfaces by Supercritical CO_2. Biomacromolecules 13 (4), 1152–1160. https://doi.org/10.1021/bm300053d.

García-González, C.A., Barros, J., Rey-Rico, A., Redondo, P., Gómez-Amoza, J.L., Concheiro, A., Alvarez-Lorenzo, C., Monteiro, F.J., 2018. Antimicrobial Properties and Osteogenicity of Vancomycin-Loaded Synthetic Scaffolds Obtained by Supercritical Foaming. ACS Appl. Mater. Interfaces 10 (4), 3349–3360. https://doi.org/10.1021/acsami.7b1737510.1021/acsami.7b17375.s001.

García-González, C.A., Concheiro, A., Alvarez-Lorenzo, C., 2015. Processing of Materials for Regenerative Medicine Using Supercritical Fluid Technology. Bioconjug. Chem. 26 (7), 1159–1171. https://doi.org/10.1021/bc5005922.

Garcia-Gonzalez, L., Geeraerd, A.H., Spilimbergo, S., Elst, K., Van Ginneken, L., Debevere, J., Van Impe, J.F., Devlieghere, F., 2007. High pressure carbon dioxide inactivation of microorganisms in foods: The past, the present and the future. Int. J. Food Microbiol. 117 (1), 1–28. https://doi.org/10.1016/j.ijfoodmicro.2007.02.018.

Goimil, L., Braga, M.E.M., Dias, A.M.A., Gómez-Amoza, J.L., Concheiro, A., Alvarez-Lorenzo, C., de Sousa, H.C., García-González, C.A., 2017. Supercritical processing of starch aerogels and aerogel-loaded poly(ε-caprolactone) scaffolds for sustained release of ketoprofen for bone regeneration. J. CO2 Util. 18, 237–249. https://doi.org/10.1016/j.jcou.2017.01.028.

Goimil, L., Jaeger, P., Ardao, I., Gómez-Amoza, J.L., Concheiro, A., Alvarez-Lorenzo, C., García-González, C.A., 2018. Preparation and stability of dexamethasone-loaded polymeric scaffolds for bone regeneration processed by compressed CO_2 foaming. J. CO2 Util. 24, 89–98. https://doi.org/10.1016/j.jcou.2017.12.012.

Goimil, L., Santos-Rosales, V., Delgado, A., Évora, C., Reyes, R., Lozano-Pérez, A.A., Aznar-Cervantes, S.D., Cenis, J.L., Gómez-Amoza, J.L., Concheiro, A., Alvarez-Lorenzo, C., García-González, C.A., 2019. scCO_2-foamed silk fibroin aerogel/poly (ε-caprolactone) scaffolds containing dexamethasone for bone regeneration. J. CO2 Util. 31, 51–64. https://doi.org/10.1016/j.jcou.2019.02.016.

Hedayati, S.K., Behravesh, A.H., Hasannia, S., Bagheri Saed, A., Akhoundi, B., 2020. 3D printed PCL scaffold reinforced with continuous biodegradable fiber yarn: A study on mechanical and cell viability properties. Polym. Test. 83, 106347. https://doi.org/10.1016/j.polymertesting.2020.106347.

Ho, S.T., Hutmacher, D.W., 2006. A comparison of micro CT with other techniques used in the characterization of scaffolds. Biomaterials 27 (8), 1362–1376. https://doi.org/10.1016/j.biomaterials.2005.08.035.

ISO 11135:2014 Sterilization of health-care products – Ethylene oxide – Requirements for the development, validation and routine control of a sterilization process for medical devices. 2014., n.d.

ISO 11137-1:2006/Amd.1:2013 Sterilization of health care products – Radiation – Part 1: Requirements for development, validation and routine control of a sterilization process for medical devices." 2006., n.d.

ISO, 2009. 14937:2009 Sterilization of health care products — General requirements for characterization of a sterilizing agent and the development, validation and routine control of a sterilization process for medical devices. International Organization for Standardization n.d.

Josephs-Spaulding, J., Singh, O.V., 2021. Medical Device Sterilization and Reprocessing in the Era of Multidrug-Resistant (MDR) Bacteria: Issues and Regulatory Concepts. Front. Med. Technol. 2, 587352 https://doi.org/10.3389/fmedt.2020.587352.

Li, B., Brown, K.V., Wenke, J.C., Guelcher, S.A., 2010. Sustained release of vancomycin from polyurethane scaffolds inhibits infection of bone wounds in a rat femoral segmental defect model. J. Controlled Release 145 (3), 221–230. https://doi.org/10.1016/j.jconrel.2010.04.002.

Li, B., Webster, T.J., 2017. Bacteria antibiotic resistance: New challenges and opportunities for implant-associated orthopedic infections: Bacteria antibiotic resistance. J. Orthop. Res. https://doi.org/10.1002/jor.23656.

López-Iglesias, C., Barros, J., Ardao, I., Gurikov, P., Monteiro, F.J., Smirnova, I., Alvarez-Lorenzo, C., García-González, C.A., 2020. Jet Cutting Technique for the Production of Chitosan Aerogel Microparticles Loaded with Vancomycin. Polymers 12, 273. https://doi.org/10.3390/polym12020273.

Makadia, H.K., Siegel, S.J., 2011. Poly Lactic-co-Glycolic Acid (PLGA) as Biodegradable Controlled Drug Delivery Carrier. Polymers 3, 1377–1397. https://doi.org/10.3390/polym3031377.

Mangir, N., Dikici, S., Claeyssens, F., MacNeil, S., 2019. Using ex Ovo Chick Chorioallantoic Membrane (CAM) Assay To Evaluate the Biocompatibility and Angiogenic Response to Biomaterials. ACS Biomater. Sci. Eng. 5 (7), 3190–3200. https://doi.org/10.1021/acsbiomaterials.9b0017210.1021/acsbiomaterials.9b00172.s001.

Martinez, L.R., Han, G., Chacko, M., Mihu, M.R., Jacobson, M., Gialanella, P., Friedman, A.J., Nosanchuk, J.D., Friedman, J.M., 2009. Antimicrobial and Healing Efficacy of Sustained Release Nitric Oxide Nanoparticles Against Staphylococcus Aureus Skin Infection. J. Invest. Dermatol. 129 (10), 2463–2469. https://doi.org/10.1038/jid.2009.95.

Moreno-Jiménez, I., Kanczler, J.M., Hulsart-Billstrom, G., Inglis, S., Oreffo, R.O.C., 2017. The Chorioallantoic Membrane Assay for Biomaterial Testing in Tissue Engineering: A Short-Term *In Vivo* Preclinical Model. Tissue Eng. Part C Methods 23, 938–952. https://doi.org/10.1089/ten.tec.2017.0186.

Premkumar, A., Kolin, D.A., Farley, K.X., Wilson, J.M., McLawhorn, A.S., Cross, M.B., Sculco, P.K., 2021. Projected Economic Burden of Periprosthetic Joint Infection of the Hip and Knee in the United States. J. Arthroplasty 36 (5), 1484–1489.e3. https://doi.org/10.1016/j.arth.2020.12.005.

Ribatti, D., 2016. The chick embryo chorioallantoic membrane (CAM). A multifaceted experimental model. Mech. Dev. 141, 70–77. https://doi.org/10.1016/j.mod.2016.05.003.

Ribeiro, N., Soares, G.C., Santos-Rosales, V., Concheiro, A., Alvarez-Lorenzo, C., García-González, C.A., Oliveira, A.L., 2020. A new era for sterilization based on supercritical CO_2 technology. J. Biomed. Mater. Res. B Appl. Biomater. 108 (2), 399–428. https://doi.org/10.1002/jbm.b.v108.210.1002/jbm.b.34398.

Richbourg, N.R., Peppas, N.A., Sikavitsas, V.I., 2019. Tuning the biomimetic behavior of scaffolds for regenerative medicine through surface modifications. J. Tissue Eng. Regen. Med. 13 (8), 1275–1293. https://doi.org/10.1002/term.v13.810.1002/term.2859.

Rochford, E.T.J., Richards, R.G., Moriarty, T.F., 2012. Influence of material on the development of device-associated infections. Clin. Microbiol. Infect. 18 (12), 1162–1167. https://doi.org/10.1111/j.1469-0691.2012.04002.x.

Santos-Rosales, V., Ardao, I., Alvarez-Lorenzo, C., Ribeiro, N., Oliveira, A., García-González, C., 2019. Sterile and Dual-Porous Aerogels Scaffolds Obtained through a Multistep Supercritical CO_2-Based Approach. Molecules 24, 871. https://doi.org/10.3390/molecules24050871.

Santos-Rosales, V., Ardao, I., Goimil, L., Gomez-Amoza, J.L., García-González, C.A., 2021a. Solvent-Free Processing of Drug-Loaded Poly(ε-Caprolactone) Scaffolds with Tunable Macroporosity by Combination of Supercritical Foaming and Thermal Porogen Leaching. Polymers 13, 159. https://doi.org/10.3390/polym13010159.

Santos-Rosales, V., Gallo, M., Jaeger, P., Alvarez-Lorenzo, C., Gómez-Amoza, J.L., García-González, C.A., 2020a. New insights in the morphological characterization and modelling of poly(ε-caprolactone) bone scaffolds obtained by supercritical CO_2 foaming. J. Supercrit. Fluids 166, 105012. https://doi.org/10.1016/j.supflu.2020.105012.

Santos-Rosales, V., Iglesias-Mejuto, A., García-González, C.A., 2020b. Solvent-Free Approaches for the Processing of Scaffolds in Regenerative Medicine. Polymers 12, 533. https://doi.org/10.3390/polym12030533.

Santos-Rosales, V., Magariños, B., Starbird, R., Suárez-González, J., Fariña, J.B., Alvarez-Lorenzo, C., García-González, C.A., 2021b. Supercritical CO_2 technology for one-pot foaming and sterilization of polymeric scaffolds for bone regeneration. Int. J. Pharm. 605, 120801. https://doi.org/10.1016/j.ijpharm.2021.120801.

Seddighian, A., Ganji, F., Baghaban-Eslaminejad, M., Bagheri, F., 2021. Electrospun PCL scaffold modified with chitosan nanoparticles for enhanced bone regeneration. Prog. Biomater. 10 (1), 65–76. https://doi.org/10.1007/s40204-021-00153-8.

Serbo, J.V., Gerecht, S., 2013. Vascular tissue engineering: biodegradable scaffold platforms to promote angiogenesis. Stem Cell Res. Ther. 4, 8. https://doi.org/10.1186/scrt156.

Shieh, E., Paszczynski, A., Wai, C.M., Lang, Q., Crawford, R.L., 2009. Sterilization of Bacillus pumilus spores using supercritical fluid carbon dioxide containing various modifier solutions. J. Microbiol. Methods 76 (3), 247–252. https://doi.org/10.1016/j.mimet.2008.11.005.

Soares, G.C., Learmonth, D.A., Vallejo, M.C., Davila, S.P., González, P., Sousa, R.A., Oliveira, A.L., 2019. Supercritical CO_2 technology: The next standard sterilization technique? Mater. Sci. Eng. C 99, 520–540. https://doi.org/10.1016/j.msec.2019.01.121.

Stone, J.R., Yang, S., 2006. Hydrogen Peroxide: A Signaling Messenger. Antioxid. Redox Signal. 8 (3-4), 243–270. https://doi.org/10.1089/ars.2006.8.243.

Tai, H., Mather, M., Howard, D., Wang, W., White, L., Crowe, J., Morgan, S., Chandra, A., Williams, D., Howdle, S., Shakesheff, K., 2007. Control of pore size and structure of tissue engineering scaffolds produced by supercritical fluid processing. Eur. Cell. Mater. 14, 64–77. https://doi.org/10.22203/eCM.v014a07.

Tipnis, N.P., Burgess, D.J., 2018. Sterilization of implantable polymer-based medical devices: A review. Int. J. Pharm. 544 (2), 455–460. https://doi.org/10.1016/j.ijpharm.2017.12.003.

Watt, B.E., Proudfoot, A.T., Vale, J.A., 2004. Hydrogen Peroxide Poisoning. Toxicol. Rev. 23, 51–57. https://doi.org/10.2165/00139709-200423010-00006.

Woodruff, M.A., Hutmacher, D.W., 2010. The return of a forgotten polymer—Polycaprolactone in the 21st century. Prog. Polym. Sci. 35, 1217–1256. https://doi.org/10.1016/j.progpolymsci.2010.04.002.

Yang, D., Wijenayaka, A.R., Solomon, L.B., Pederson, S.M., Findlay, D.M., Kidd, S.P., Atkins, G.J., 2018. Novel Insights into *Staphylococcus aureus* Deep Bone Infections: the Involvement of Osteocytes. mBio 9, e00415-18, /mbio/9/2/mBio.00415-18.atom. https://doi.org/10.1128/mBio.00415-18.

Zhang, J., Burrows, S., Gleason, C., Matthews, M.A., Drews, M.J., LaBerge, M., An, Y.H., 2006a. Sterilizing Bacillus pumilus spores using supercritical carbon dioxide. J. Microbiol. Methods 66, 479–485. https://doi.org/10.1016/j.mimet.2006.01.012.

Zhang, J., Dalal, N., Gleason, C., Matthews, M.A., Waller, L.N., Fox, K.F., Fox, A., Drews, M.J., LaBerge, M., An, Y.H., 2006b. On the mechanisms of deactivation of Bacillus atrophaeus spores using supercritical carbon dioxide. J. Supercrit. Fluids 38 (2), 268–273. https://doi.org/10.1016/j.supflu.2006.02.015.

Zhang, J., Davis, T.A., Matthews, M.A., Drews, M.J., LaBerge, M., An, Y.H., 2006c. Sterilization using high-pressure carbon dioxide. J. Supercrit. Fluids 38 (3), 354–372. https://doi.org/10.1016/j.supflu.2005.05.005.

Zhao, Y., Zhu, B.o., Wang, Y., Liu, C., Shen, C., 2019. Effect of different sterilization methods on the properties of commercial biodegradable polyesters for single-use, disposable medical devices. Mater. Sci. Eng. C 105, 110041. https://doi.org/10.1016/j.msec.2019.110041.